INVESTIGATION OF THERMAL AND DIMENSIONAL BEHAVIOR OF 3-D PRINTED MATERIALS USING THERMAL IMAGING AND 3-D SCANNING

by

Zorana Z. GOLUBOVIĆ[a*], Milan N. TRAVICA[b], Isaak D. TRAJKOVIĆ[b], Aleksandar Lj. PETROVIĆ[a], Žarko Z. MIĆKOVIĆ[a], and Nenad R. MITROVIĆ[a]

[a] Faculty of Mechanical Engineering, University of Belgrade, Belgrade, Serbia
[b] Innovation Center of Faculty of Mechanical Engineering, Belgrade, Serbia

Original scientific paper
https://doi.org/10.2298/TSCI2301021G

Fused deposition modeling is one of the most widely used 3-D printing technologies, among other additive manufacturing processes, because it is easy to use, can produce parts faster, and the cost of the finished part is low. Printing processes and finished parts are often studied and characterized using different techniques to collect mechanical, numerical, thermal and dimensional data, with the aim of improving and optimizing the result. The first part of this research is based on the observation of temperature changes with a thermal imaging camera during the fused deposition modeling printing process and during the cooling process after printing. Specimens of polylactic acid and polylactic acid-X improved with second-phase particles were prepared to compare the thermal and dimensional properties of the two materials. The obtained results determined the characteristic temperature behavior of the materials. In the second part of the research, a 3-D optical-scanner was used to verify the stability and accuracy of the printed specimens over time. The proposed measurement period showed that stabilization of the parameters takes place, and further follow-up should be performed thereafter.

Key words: *fused deposition modeling, polylactic acid, polylactic acid-X, thermal imaging, temperature changes, 3-D scanning, dimensional accuracy*

Introduction

The past decades have been significant for the development of additive manufacturing (AM) technologies. According to the ISO/ASTM standard AM technologies are described as processes for building up materials layer-by-layer. Seven types of AM processes are represented in the standard, *i.e.*, vat photopolymerization, material extrusion, direct energy deposition, material jetting, binder jetting, sheet lamination, and powder bed fusion. These technologies are also referred to as rapid prototyping (RP), solid free-form (SFF) technology, or 3-D printing [1, 2]. Each type has a several subtypes leading to many possibilities in various AM processes, as well as in different areas of industry and medical sciences [3, 4]. These technologies offer new opportunities and greater freedom in design, the final products have improved mechanical properties and customizable geometries, the manufacturing process is faster, and

* Corresponding author, e-mail: zzgolubovic@mas.bg.ac.rs

the production costs are lower [4, 5]. Various materials are used in 3-D printing processes, from polymers, to polymer composites, various thermoplastics, graphene-based materials, metals, alloys, and concrete [6, 7].

Among the other AM processes mentioned, fused deposition modeling (FDM) is one of the most frequently used 3-D printing technologies, because of its ease of use, high production speed and low cost of the finished part [6]. The FDM process begins with the preparation of the file (product) which is printed in the CAD software in stereolithography (STL) format. Then the layers are built up from the bottom to the top [8], where the material in the form of a continuous filament is generated by a hot nozzle and applied under pressure when the layers of parts are formed [3, 9]. The temperature of the filament during the extrusion process is beyond the crystalline melting temperature, T_m, *i.e.*, the glass transition temperature, T_g, and after a layer is extruded on the heated bed or on the previous layer, another layer is reheated and extruded on top of it, followed by the cooling process when the extruded filaments solidify and form the solid geometry [10, 11]. Numerous research studies deal with AM processes and the control and monitoring of various parameters in the printing process, but fewer studies deal with the monitoring and control of FDM 3-D printing processes [12]. The mechanical properties of printed parts depend on the process parameters [13], which include material selection, layer thickness, infill density, raster angle and width, build orientation, nozzle temperature and printing speed [3, 14]. Studies have shown that low layer thickness and high infill densities result in better surface finish, while high layer thickness and high infill densities result in improved dimensional accuracy. A deterioration of the mechanical properties is observed with decreasing infill density [2]. Another feature that should be taken into account is the fact that FDM is a purely thermal process and it is important to include thermal analysis in the 3-D printing process and parameter verification.

The main materials used for FDM processes are thermoplastic polymeric materials: polylactic acid (PLA), acrylonitrile butadiene styrene (ABS), thermoplastic polyurethane (TPU), polyethylene terephthalate (PET), and these materials are also used as reinforced with different types of particles to improve their properties. In this study PLA and an advanced PLA material with an addition of second-phase particles, *i.e.*, PLA-X were used. The PLA has many advantages in printing processes, as that it has very good thermoformability at low processing temperatures compared to other polymers and crystalizes quickly after cooling. Due to the confirmed disadvantages, such as lack of thermal stability, degradation behavior and brittleness, PLA has been filled with different particles and materials, *e.g.*, nanoparticles, carbon whiskers, wood flour [15]. Printing parameters and behavior of PLA in terms of mechanical and thermal behavior have been thoroughly studied for years. On the other hand, PLA-X has been shown to have better mechanical properties and higher dimensional accuracy during printing compared to PLA material [16].

Evolution of the temperature during the printing process depends on the thermal parameters of the environment, the build platform, the nozzle temperature on one side, and on the other, printing parameters such as printing speed, layer height, and width of the printed specimen are also important [5]. Control of these thermal and mechanical properties is important for improving the quality and accuracy of the FDM process and final products [17-20]. The heating and cooling cycles during the printing process affect the formation of bonds, which ultimately affect the final mechanical properties, dimensional accuracy, and quality of the 3-D printed part in terms of deformation, warpage, voids *etc.*, as mentioned previously [21-24]. Therefore, it is beneficial to track the temperature changes during the printing process and scan the geometry afterwards.

Various techniques have been used for temperature measurements and characterization of polymer AM processes. The types of techniques vary depending on the 3-D printing processes used. Temperature behavior has been observed using thermocouples, thermal/infrared cameras, high-speed cameras, X-rays, *etc.* [4, 18, 20, 25].

Thermal imaging is non-contact, non-invasive measurement technique in which radiometers register infrared radiation and thermal energy from the surface of the observed object in the form of beams [26], which provides high efficiency and better safety compared to conventional testing and monitoring technologies [27, 28]. The high thermal sensitivity and low spatial resolution of the cameras allow monitoring thermal changes at different printing settings with different materials. The temperature of the polymer during extrusion affects the thermal shrinkage during the process when cooling from the liquid temperature to the temperature of the processed parts [29]. This can be controlled by adjusting the printer chamber and build plate temperature [24]. Some studies have explained the effect of thermal progression on dimensional accuracy by observing the printing temperature, temperature distribution during printing, layer height, and cooling of the printed part and noting the deformations that occur [17, 30, 31].

The accuracy of 3-D printed parts includes dimensional accuracy, geometric accuracy and surface roughness, *i.e.*, the printed part is compared with the digital model and all prescribed parameters [29]. In addition, the dimensions and geometric accuracy of printed parts may change over time after printing [32]. In order to perform such measurements non-contact *optical 3-D scanners* are used, at a specific point in time. Optical 3-D scanning systems process the light on the observed part, digitize it, and obtain millions of points of reflected light as a result, which are numerically processed in the corresponding software [33].

The aim of this research was to analyze the temperature change during the 3-D printing process of PLA and PLA-X specimens, and to verify the accuracy and stability of the printed specimens over time.

Methodology

Materials

Two commercially available thermoplastic polymers were used in this study: PLA (RepRap, Germany) and improved polylactic acid (PLA-X) (mcPP, Mitsubishi Chemical, Japan). The PLA is a biodegradable, non-toxic organic polymer derived from bio-based resources. This material has good dimensional stability and is easy to extrude at low temperatures, so the platform does not need to be heated. It melts at lower temperatures of 180-220 °C and has a glass transition temperature in the range of 60-65 °C [34]. There are some problematic properties of PLA, including thermal resistance which also affect the mechanical properties. Improvement of some PLA properties is possible by adding polymer blends, composites or second-phase particles into polymer matrix. The PLA-X used in this study is the advanced version of PLA with incorporated second-phase particles and a melting temperature of 190-220 °C [35]. Both materials consisted of filaments with a diameter of 1.75 mm.

Experimental procedure

Specimen preparation – 3-D printing

The specimens used in this study were fabricated in SolidWorks CAD software, with dimensions of 10 × 5 × 5 mm, fig. 1. For each material, 5 specimens were made.

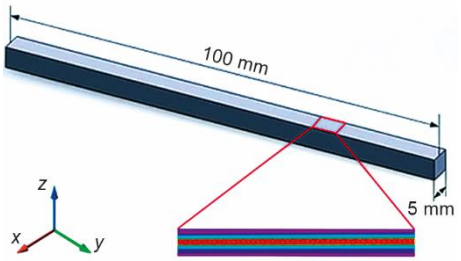

Figure 1. The 3-D CAD image of test specimen and its infill pattern

The specimens were printed using the RepRap X400 (Rep Rap, Germany) 3-D printer. Infill pattern for all samples was concentric with 30% of infill density. The layer height was 0.2 mm, with 2 layers on top, 2 on bottom and 2 from both sides. The nozzle temperature was set to an average of 195.5 °C, the nozzle diameter to 0.4 mm, and the printing speed was 60 mm/s. The temperature of the printing chamber was 33.2 °C, and the temperature of the platform was 48.1 °C.

Before starting the printing process the specimens were placed 5.5 cm from the edge of the printer, and after the printing process was completed the specimens were not post-processed.

Thermal analysis

These experiments were performed using the PeakTech 5620 (PeakTech, Germany) thermal imaging camera, which was placed at an optimal distance of 30 cm from the sample. The camera was placed on an adjustable tripod that provided constant position and stability with respect to the platform of the printer and recorded the specimen throughout the experiment. The door of the 3-D printer was open, as the Plexiglas would prevent the capture of the printing space. The temperature was kept constant at 23 °C by air-conditioning, and the humidity was 55% RH. For the measurements, the emissivity of the printed material was set at 0.92 [36].

The camera recorded raw data in the form of videos and images for the determined position in real time, and thus temperature data were obtained for each point of the observed specimen. Further details of the thermal imaging camera used are given in tab. 1.

Table 1. Characteristics of thermal imaging camera PeakTech 5620 [37]

Temperature range	–20 °C to +550 °C
Accuracy	± 2% ± 2 °C
Thermal resolution	384 × 288 pixels
Field of view (FOV)	37.2° × 28.5°
Spectral range	8-14 µm
Image frequency	25 Hz
Emissivity	0.01-1.0

The camera is set to face the front of the printing platform where the printed specimen is located in the center of the platform, fig. 2(a). The areas of interest, *i.e.*, the observed lines on the specimens are set by the software on the captured images, fig. 2(b).

Images were taken at the beginning of printing, and every 10 seconds during printing. After printing was finished, images were taken every 10 seconds for a period of 1 minute.

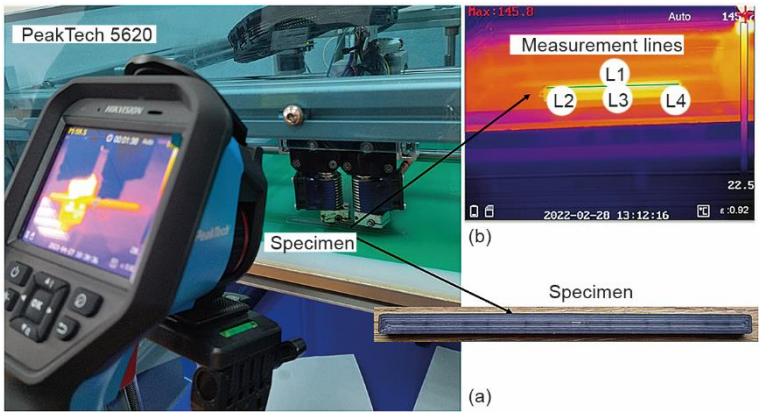

Figure 2. Experimental set-up showing RepRap X400 printer printing specimen and PeakTech 5620 thermal camera recording during 3-D printing process with measurement lines

The 3-D scanning

Specimens were placed in the 3-D scanner sequentially at a precisely defined time period, *i.e.*, specimens were allowed to cool for 5 minutes after printing, then each specimen was removed from the platform and for the next 5 minutes they were prepared and positioned for scanning. Atos Core 200 (GOM, Braunschweig, Germany) non-contact optical scanner with GOM Inspect software (data acquisition software of scanner) was used to investigate geometry changes, tab. 2. The same environmental conditions were maintained throughout the scanning of the specimens, *i.e.*, a constant temperature of 23 ℃ with air-conditioning and humidity of 55% RH.

Table 2. Characteristics of optical 3D scanner Atos Core 200 [38].

Measuring area	200 × 150 mm
Working distance	250 mm
Sensor dimensions	206 × 205 × 64
Temperature range	5 °C to +40 °C, non-condensing
Point density	0.08 mm

Atos 3-D Scanner represents a system for optical measurements based on optical triangulation, fringe projection and photometry. Observed measured objects are quickly digitized, achieving relatively high precision and resolution. The 3-D scanner, fig. 3, has a projector with configured sensors for the area to be measured and a computer-controlled turntable that allows the object to be positioned in all desired planes [32].

Each 3-D scanned model overlaps with the corresponding model from CAD. The goal was to observe the discrepancies between the CAD model and the 3-D scanned specimen. These scans were also performed at a specific time, every day after exactly 24 hours in a period of 7 days. The aim of this study was also to determine the influence of time on the change of the specimen geometry.

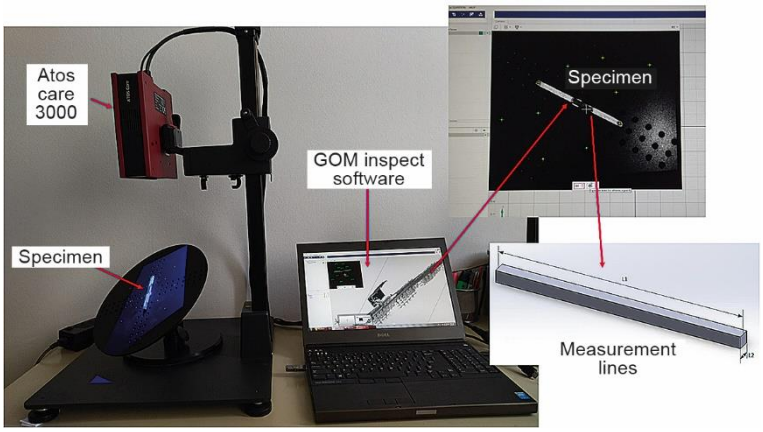

Figure 3. Experimental set-up of 3-D scanning process with specimen model and measurement lines

Results and discussions

Thermal imaging

Thermo-visual measurements were performed to track the temperature distribution during 3-D printing. The acquisition of thermal data is based on the infrared signals which depend on the emissivity of the material [11]. The 3-D printing process was monitored using the Thermal Imaging iVMS-4800 software, and the temperature profiles of the specimens were recorded for each newly deposited layer. The temperature profile shows the average temperature in a given region of interest, *i.e.*, the temperature distribution on the surface of a deposited layer.

Thermal imaging camera images show different colors depending on the position of the print nozzle which is the hottest area from which the polymer is directly extruded. Color changes occur as the filaments begin to solidify and range from yellow to orange to red. At lower temperatures colder colors appear, pink, purple, and blue. The average temperature of the top layer depends on the rate of cooling. The area in which the printer's nozzle prints the material onto the previously applied layer has a direct influence on the surface temperature of the layers.

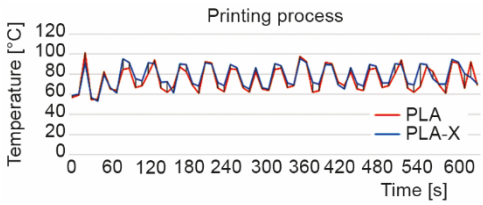

Figure 4. Software presentation of thermal evolution during printing process of PLA and PLA-X materials

The temperature values for the two materials PLA and PLA-X are shown as average values over time, fig. 4. From the figures, it can be seen that the trend of the diagram resembles a sinusoidal function and that the measured temperature values on the surface of the specimen are approximately the same at each moment. It can be concluded that the temperature changes during the printing process are identical for both materials. In this respect, a different thermal performance of the PLA-X material with improved properties due to the addition of the second-base particles, is not evident.

During the cooling process, the temporal temperature changes are approximately linear for all measurement lines. The initial difference in the diagram for measurement line L1 is the result of the increased residual temperature in the last part of the printing, fig. 5. The temperature value is higher at this point, while after 20 seconds it stabilizes and approaches the average temperatures of the other measurement lines. The cooling process was analyzed in the period of 60 seconds after the end of the printing because in this period the temperature changes are the most significant.

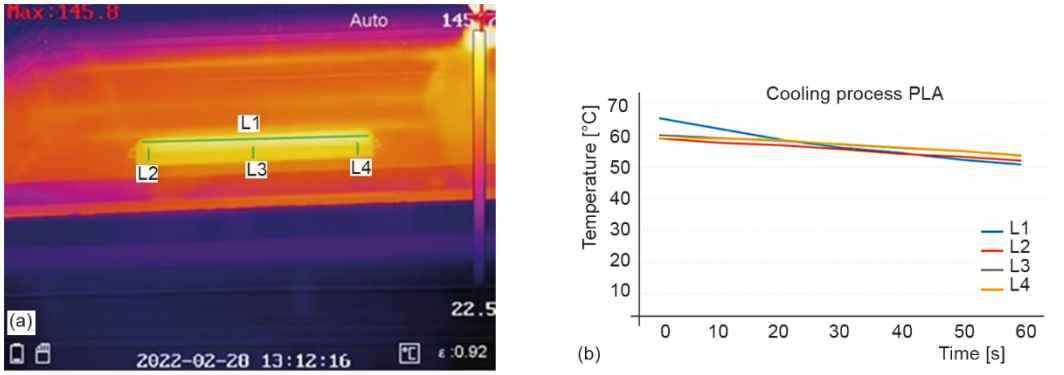

Figure 5. Temperature profile of colling process in period of 60 seconds for specimens of PLA material

The diagram for the cooling process of the PLA-X specimens shows that the temperature changes are approximately linear for all measurement lines, fig. 6. The initial difference, as with the PLA specimens, is the result of the increased residual temperature in the final phase of the printing process. The stabilization of the temperature, which is stlightly higher at the beginning, occurs after 17 seconds and approaches the average values for all other measurement lines.

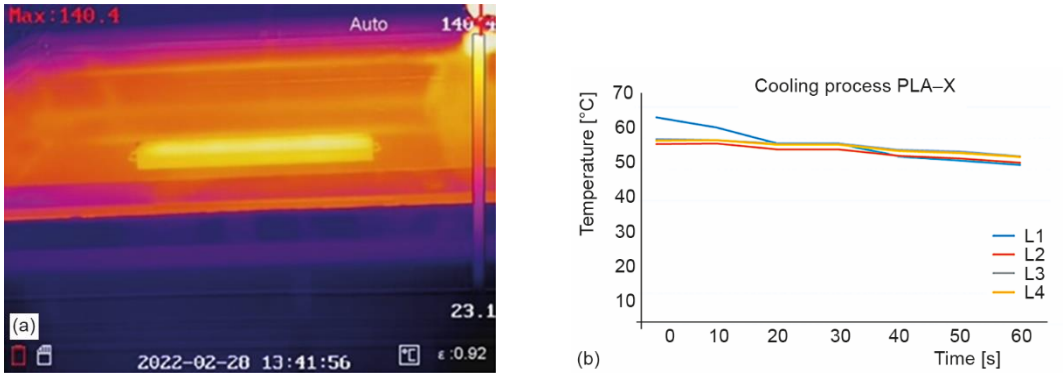

Figure 6. Temperature profile of colling process in period of 60 seconds for specimens of PLA-X material

Temperatures at the surface of the specimen are accurate, but there are slight limitations in detecting temperatures in all layers of the printed specimen. When observing the

printing process, the upper layers of the specimen are hot after extrusion, and cooling is slow because the heat zone is small. Another fact that should be taken into account is that the printing platform is constantly heated during the printing process and also after the printing process is finished, which affects the temperature of the sample at every moment that the sample is on the platform. Previous studies concluded that the temperature distribution on the specimens is not uniform and that a constant gradient cannot be formed [39].

The 3-D scanning

The 3-D scanner's projector with its configured sensors measures the 3-D area of the scanned specimen and displays the specimen's measurement volume. Since the scanned 3-D model was not complete and smaller parts of the measurement volume were missing, errors will occur during further measurement of accuracy and control of length. It can be seen from the diagram that the length of the specimen has a decreasing trend, fig. 7. The values for the PLA-X specimen have more pronounced peaks due to the incomplete model of the scanned surface. The diagram for the PLA specimen clearly shows that there is no difference in the length of the specimen from day 5 to day 7, leading to the conclusion that the value becomes stable.

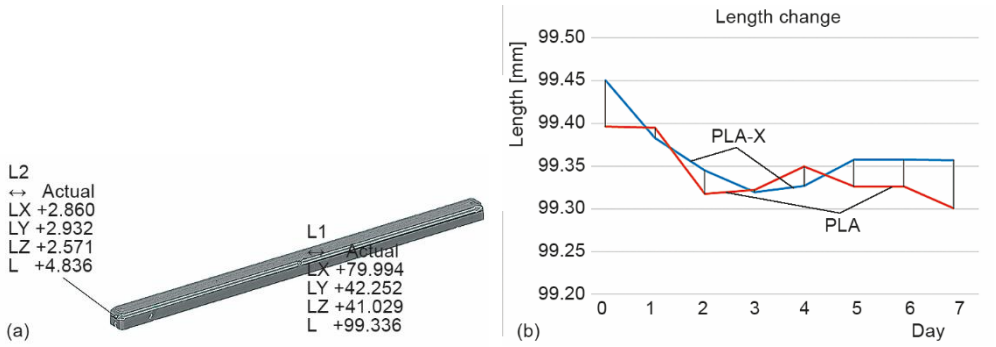

Figure 7. Length change od specimens over period of one week

The diagram for the width changes of the specimens shows that the changes occur in the first 4 days after the end of the-printing process, and after that the width changes are negligible, fig. 8. Again, there are slight inconsistencies due to an incomplete model of the scanned surface of the specimen. The incompleteness of the model is related to missing parts, as mentioned before, which in turn can lead to minor errors in the measurement of the width of the specimens.

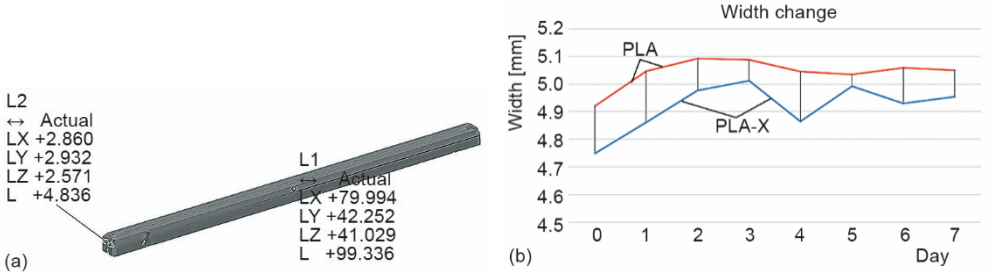

Figure 8. Width change od specimens over period of one week

As the parameters stabilize in the first week after printing, the authors recommend reducing the scanning frequency for measuring the geometry and dimensional accuracy of printed samples.

Conclusions

Analyzing the effects of temperature variations in 3-D printing is important because it is a thermal process. Once the printing process is complete, it is also important to track the geometric parameters to determine if the printed specimen matches to the model created in the CAD software.

In this paper, thermal and dimensional analyzes of 3-D printed specimens were presented. The main objective of this research was to determine how the temperature changes during and after the completion of the 3-D printing process of PLA and PLA-X specimens, and to observe dimensional accuracy and stability of the printed specimens over a period of one week. For this purpose, the in-situ thermal imaging monitoring technique was used to track the thermal evolution during the manufacturing process. The experiments have shown the approximate temperature values measured on the surface of the specimens for each moment. The addition of second-base particles to the PLA-X material did not affect the temperature evolution compared to PLA. Therefore, it is concluded that there were no differences between PLA and the PLA-X reinforced material in terms of the temperature changes during printing and cooling process. In the second part of this study, all the specimens were scanned with a 3-D scanner to determine any changes in dimensions from the original model. Inconsistencies in the obtained model of the scanned surface of the specimens affected the diagrams due to minor errors in the measurement of the length and width of the specimens. A decreasing trend is observed in the length of the specimens. Due to the incomplete scanned models, the peaks are more pronounced in the PLA-X samples, and in the PLA samples the stabilization of the geometry occurred around the fifth day. It is recommended that dimensional control should be performed after this period to optimize the process. The literature search revealed a limited number of research papers that addressed the characterization of the specimens in a manner described in this paper.

Future research will include thermal observations of various parameters during the 3-D printing process, *i.e.*, changing infill pattern and infill percentage, and using different materials. In 3-D scanning, measurement of dimensional accuracy should be done in a longer aging period due to stabilization of parameters in the first week after printing.

Acknowledgment

This research was financially supported by the Ministry of Education, Science and Technological Development of the Republic of Serbia by Contract No. 451-03-68/2022-14/200105 from 4.2.2022.

References

[1] Evans, B., *Practical 3D Printers*, Paul Manning, New York, USA, 2012
[2] Abeykoon, C., *et al.*, Optimization of Fused Deposition Modeling Parameters for Improved PLA and ABS 3D Printed Structures, *International Journal of Lightweight Materials and Manufacture*, *3* (2020), 3, pp. 284-297
[3] Arefin, A. M. E., *et al.*, Polymer 3D Printing Review: Materials, Process, and Design Strategies for Medical Applications, *Polymers*, *13* (2021), 9, ID 1499
[4] Borish, M., A Survey of Thermal Sensing Application in Additive Manufacturing, *Proceedings,* SPIE 11743, Thermosense: Thermal Infrared Applications XLIII, 117430A, 12 April 2021

[5] Garzon-Hernandes, S., *et al*., Design of FDM 3D Printed Polymers: An Experimental-Modelling Methodology for the Prediction of Mechanical Properties, *Materials and Design 188* (2020), Mar., ID 108414
[6] Ngo, T. D., *et al.*, Additive Manufacturing (3D printing): A Review of Materials, Methods, Applications and Challenges. *Compos. Part B Eng*., *143* (2018), June, pp. 172-196
[7] Yuan, Y., *et al.*, Prediction of Temperature and Crystal Growth Evolution During 3D Printing of Polymeric Materials via Extrusion., *Materials and Design, 196* (2020), Nov., ID 109121
[8] Ariffin, M. M., *et al.*, Slicer Method Comparison Using Open-Source 3D Printer, *Proceedings,* IOP Conference Series: Earth and Environmental Science, IOP Publishing, *114* (2018), 012018
[9] Dong, G., *et al.*, Optimizing Process Parameters of Fused Deposition Modeling by Taguchi Method for the Fabrication of Lattice Structures, *Additive Manufacturing, 19* (2018), Jan., pp. 62-72
[10] Dinwiddie R. B., *et al.*, Infrared Imaging of the Polymer 3D-Printing Process, *Proceedings,* SPIE 9105, Thermosense: Thermal Infrared Applications XXXVI, Bellingham, Wash., USA, 2014, pp. 910502
[11] Seppla, J. E., Migler, K. D., Infrared Thermography of Welding Zones Produced by Polymer Extrusion Additive Manufacturing, *Additive Manufacturing, 12* (2016), Part A, pp. 71-76
[12] Malekipour, E., *et al.*, Investigation of Layer Based Thermal Behavior in Fused Deposition Modelling Process by Infrared Thermography, *Procedia Manufacturing, 26* (2018), Jan., pp. 1014-1022
[13] Chalgham A., *et al.*, Mechanical Properties of FDM Printed PLA Parts before and after Thermal Treatment, *Polymers*, *13* (2021), 8, ID 1239
[14] Kaveh M., *et al*. Optimization of the Printing Parameters Affecting Dimensional Accuracy and Internal Cavity for HIPS Material Used in Fused Deposition Modeling Processes, *J. Mater. Process. Technol. 226* (2015), Dec., pp. 280-286
[15] Guessasma S., *et al.*, On the Tensile Behaviour of Bio-Sourced 3D-Printed Structures from a Microstructural Perspective, *Polymers, 12* (2020), 5, ID 1060
[16] Milovanović A., *et al*., Influence of Second-Phase Particles on Fracture Behaviour of PLA and Advanced PLA-X Material, *Procedia Structural Integrity, 31* (2021), 9-10, pp. 122-126
[17] Geng, P., *et al*., Effect of Thermal Processing and Heat Treatment Condition on 3D Printing PPS Properties, *Polymers, 10* (2018), 8, ID 875
[18] Ravoori, D., *et al*., Investigation of Process-Structure-Property Relationships in Polymer Extrusion Based Additive Manufacturing through In Situ High Speed Imaging and Thermal Conductivity Measurements, *Additive Manufacturing 23* (2018), Oct., pp. 132-139
[19] Prajapati, H., *et al*., Measurement of Anisotropic Thermal Conductivity and Inter-Layer Thermal Contact Resistance in Polymer Fused Deposition Modeling (FDM), *Additive Manufacturing 21* (2018), May, pp. 84-90
[20] Prajapati H., *et al*., Measurement of the In-Plane Temperature Field on the Build Plate During Polymer Extrusion Additive Manufacturing Using Infrared Thermometry, *Polymer Testing 92* (2020), Dec., ID 106866
[21] Garg, A., *et al*., Failure Investigation of Fused Deposition Modelling Parts Fabricated at Different Raster Angles under Tensile and Flexural Loading, *Proceedings of the Institution of Mechanical Engineers, Part B: Journal of Engineering Manufacture, 231* (2015), 11, pp. 2031-2039
[22] Faes, M., *et al*., Influence of Inter-Layer Cooling Time on the Quasi-Static Properties of ABS Components Produced via Fused Deposition Modelling, *Procedia CIRP, 42* (2016), Dec., pp. 748-753
[23] Kousiatza C., *et al*., Temperature Mapping of 3D Printed Polymer Plates: Experimental and Numerical Study, *Sensors, 17* (2017), 3, ID 456
[24] Lalegani Dezaki, M., *et al*., An Overview of Fused Deposition Modelling (FDM): Research, Development and Process Optimisation, *Rapid Prototyping Journal, 27* (2021), 3, pp. 562-582
[25] Phan D. D., *et al*., Rheological and Heat Transfer Effects in Fused Filament Fabrication, *J. Rheol., 62* (2018), 5, pp. 1097-1107
[26] Mantecon, R., *et al*., Experimental Assessment of Thermal Gradients and Layout Effects on the Mechanical Performance of Components Manufactured by Fused Deposition Modeling, *Rapid Prototyping Journal, 28* (2022), 8, pp. 1598-1608
[27] Tang, Q. J., *et al*., Experimental Research on YSZ TBC Structure Delamination Defect Detection Using Long-Pulsed Excitation of Infrared Thermal Wave Non-Destructive Testing, *Thermal Science, 23* (2019), 3A, pp. 1313-1321
[28] Tang, Q. J., *et al*., Theoretical Study on Infrared Thermal Wave Imaging Detection of Semiconductor Silicon Wafers with Micro-Crack Defects, *Thermal Science, 24* (2020), 6B, pp. 4011-4017

[29] Ciotti, M., *et al*., A Review of the Accuracy of Thermoplastic Polymeric Parts Fabricated by Additive Manufacturing, *Rapid Prototyping Journal, 28* (2022), 2, pp. 358-389
[30] Polak, R., *et al*., Determination of FDM Printer Settings with Regard to Geometrical Accuracy, Annals of DAAAM, *Proceedings,* International DAAAM Symposium, Zadar, Croatia, 2017, pp. 561-566
[31] Akter, M. S., Kabir, M. H., Temperature Optimization of RepRap (Replicating Rapid-Prototyper) 3D Printer, *Proceedings,* International Conference on Computer, Communication, Chemical, Material and Electronic Engineering (IC4ME2), IEEE, 2018, pp. 1-4
[32] Mantada P., *et al*., Parameters Influencing the Precision of Various 3D Printing Technologies, *MM Science Journal, 5* (2017), Dec., pp. 2004-2012
[33] Yalçinkaya, S., *et al*., Optical 3D Scanner Technology, *International Journal of 3D Printing Technologies and Digital Industry, 3* (2019), 1, pp. 67-75
[34] ***, German RepRap, Official Website of the Manufacturer. Available online: https:// https://reprap. world (accessed on 25 May 2022)
[35] ***, mCPP Official Website of the Manufacturer. Available online: https://mcpp-3dp.com (accessed on 25 May 2022)
[36] Morgan, R. V., *et al*., Emissivity Measurements of Additively Manufactured Materials, Report LA-UR-17-20513, Los Alamos National Laboratory, Los Alamos, N. Mex., USA, 2017
[37] ***, PeakTech WorldWide – RCE, Official Website of the Manufacturer. Available online: https://peaktech-rce.com/en/ (accessed on 25 May 2022)
[38] ***, ATOS Core scanner by GOM, Official Website of the Manufacturer. Available online: https://www.gom.com/en/products/3d-scanning?keyword=atos%20%2Bcore%20%2B200&device=c&network=g&gclid=CjwKCAjwp7eUBhBeEiwAZbHwkWgccIIlcemq91NnkpE0UCMlEaFF9SNRuMKNBr-wNyBy-RutejLQfxoCLwkQAvD_BwE (accessed on 25 May 2022)
[39] Zgryza, L., Raczynska, A. Thermovisual Measurements of 3D Printing of ABS and PLA Filaments, *Adv. Sci. Technol. Res. J., 12* (2018), 3, pp. 266-271

Paper submitted: July 4, 2022
Paper revised: November 3, 2022
Paper accepted: November 4, 2022